ADVANCING GEOLOGICAL CARBON STORAGE MONITORING WITH 3D DIGITAL SHADOW TECHNOLOGY

Abhinav Prakash Gahlot

Georgia Institute of Technology

Rafael Orozco

Georgia Institute of Technology

Felix J. Herrmann

Georgia Institute of Technology

January 24, 2025

1 Introduction

To limit global warming and achieve climate goals, the IPCC highlights the need for technologies capable of removing gigatonnes of CO_2 annually (IPCC, Panel on Climate Change) (2018)), with Geological Carbon Storage (GCS) playing a key role in this effort. GCS captures CO_2 emissions and stores them in deep geological formations. As a scalable solution for net-negative emissions (Ringrose 2020, 2023), GCS is considered essential for reducing anthropogenic CO_2. Its safety depends on accurate monitoring of subsurface CO_2 flow and its long-term behavior. Advanced time-lapse seismic imaging is particularly crucial for tracking CO_2 migration, detecting leaks, optimizing operations, and ensuring the integrity of storage sites.

A Digital Shadow (Gahlot et al. 2024) is a framework for monitoring CO_2 storage projects. It integrates field data from sources such as seismic and borehole well measurements to track changes in CO_2 saturation over time. This framework updates a digital model of the CO_2 using machine learning-assisted data assimilation techniques (Spantini, Baptista, and Marzouk 2022; Gahlot et al. 2024), including generative AI and nonlinear ensemble Bayesian filtering. By employing a Bayesian approach, it addresses uncertainties in reservoir properties, such as permeability, and incorporates this lack of information into uncertainties of plume predictions.

Compared to 2D monitoring, 3D monitoring is critical for accurately assessing and controlling GCS projects, as it provides a detailed, spatially accurate representation of induced changes in the subsurface. In GCS projects, CO_2 injection and plume migration occur in three dimensions, making 3D seismic imaging and reservoir modeling essential for capturing the full extent of CO_2 behavior. This abstract extends the uncertainty-aware 2D Digital Shadow framework (Gahlot et al. 2024) by incorporating 3D seismic imaging and 3D reservoir modeling to improve decision-making and mitigate risks associated with subsurface storage.

2 Methodology

To develop an uncertainty-aware 3D digital shadow, we follow the formulation in Gahlot et al. (2024) for the plume dynamics and observation models,

$$
\begin{aligned}
\mathbf{x}_k &= \mathcal{M}_k\big(\mathbf{x}_{k-1}, \boldsymbol{\kappa}_k; t_{k-1}, t_k\big) \\
&= \mathcal{M}_k\big(\mathbf{x}_{k-1}, \boldsymbol{\kappa}_k\big), \ \boldsymbol{\kappa}_k \sim p(\boldsymbol{\kappa}) \quad \text{for} \quad k = 1 \cdots K.
\end{aligned}
\tag{1}
$$

where $\mathbf{x}_k$ is the time-varying spatial distribution for the CO_2 saturation and pressure perturbation measured at time instants $k = 1 \cdots K$, $\mathcal{M}_k$ represents multi-phase fluid-flow simulations that transition the state from the previous timestep, t_{k-1}, to the next timestep, t_k, for all K time-lapse timesteps. The symbol $\boldsymbol{\kappa}$ represents the spatial distribution of the permeability, which is highly heterogeneous (Ringrose 2020, 2023), and is assumed to be known only in terms of its statistical distribution $p(\boldsymbol{\kappa})$. To incorporate this lack of knowledge, every time the dynamics operator is applied new samples of the subsurface permeability distribution, $\boldsymbol{\kappa} \sim p(\boldsymbol{\kappa})$ are sampled while the CO_2 saturation and reservoir pressure perturbations, collected at the previous timestep $k-1$ in the vector, $\mathbf{x}_{k-1}$, are advanced to the next timestep, $\mathbf{x}_k$.

While the dynamics can be accurately modeled through reservoir simulations, relying solely on such simulations is impractical due to the inherent stochasticity of the permeability, which remains poorly constrained. To enhance estimates of CO_2 plume behavior, real-time monitoring is essential. Time-lapse data from 3D surface seismic measurements (Lumley 2010) provide critical information, which we incorporate into our characterization of the CO_2 plumes. These time-lapse datasets are integrated within a framework designed to better capture the state of CO_2 plume, accounting for the uncertainties in the subsurface reservoir properties. The seismic datasets are modeled as

$$
\mathbf{y}_k = \mathcal{H}_k(\mathbf{x}_k) + \boldsymbol{\epsilon}_k, \ \boldsymbol{\epsilon}_k \sim p(\boldsymbol{\epsilon}) \quad \text{for} \quad k = 1, 2, \cdots, K
\tag{2}
$$

where $\mathbf{y}_k$ represents the 3D seismic data at timestep k and $\boldsymbol{\epsilon}_k$ is colored Gaussian noise added to the seismic shot records prior to reverse-time migration. To assimilate the fluid-flow simulations and the time-lapse seismic images, we use a nonlinear Bayesian filtering framework, using neural posterior density estimation to approximate the posterior distribution of the CO_2 plume state conditioned on the time-lapse seismic data. This approach leverages advanced techniques from sequential Bayesian inference and amortized neural posterior density estimation (Papamakarios et al. 2021) in a principled manner. To estimate the posterior distribution of the CO_2 plume given seismic observations, we use conditional Normalizing Flows (CNFs) (Gahlot et al. 2024). In this simulation-based framework, we carry out simulations of the state dynamics and observations (cf. equations 1 and 2) and train the CNFs on these pairs.

3 Synthetic case study

To test our method, we use a synthetic 3D Earth model from the Compass model (E. Jones et al. 2012) representative for the North Sea. We select a subset of the Compass model that includes subsurface structures suitable for CO_2 injection. The studied subset spans a physical size of 3.2 km³, discretized into a grid of dimensions $128 \times 128 \times 128$. To initialize the probabilistic digital shadow, we require an initial ensemble of potential plume scenarios. Since the reservoir properties of the CO_2 storage sites are unknown, we establish a probabilistic baseline for the 3D permeability properties of the site and use this distribution to create the plume initialization. This permeability distribution is derived by first performing probabilistic 3D full-waveform inference (Orozco, Siahkoohi, et al. 2024) on the site, assuming a baseline seismic survey was conducted prior to injection. The resulting distribution of the unknown acoustic velocity models is then converted into 128 permeability samples using the empirical relationship described in Gahlot et al. (2024).

3.1 Multi-phase flow simulations

The flow simulations are carried out using an open-source tool, JutulDarcy JutulDarcy.jl (Møyner, Bruer, and Yin 2023). Initially, the reservoir is filled with brine, and then supercritical CO_2 is injected at the rate chosen such that the storage capacity of the reservoir rocks does not exceed 3%. The injection depth is approximately $1130m$. The simulation is performed over a 4-year interval for each time-step, t_k. It outputs predicted CO_2 saturation for each of the $N = 128$ ensemble members. One of the training (predicted) saturations is shown in Figure 1(c).

3.2 Seismic simulations

The output from the 128 flow simulations are converted to changes in the subsurface acoustic properties using the Patchy saturation model (Gahlot et al. 2024). To monitor these acoustic changes, we shoot 4D seismic surveys using 16000 receivers and 16 sources with a dominant frequency of 24 Hz and a recording length of 3 sec. We added 18 dB

SNR of colored Gaussian noise to the shot records. The nonlinear wave simulations and imaging are performed using the open-source software package JUDI.jl (Witte et al. 2019; Louboutin et al. 2023).

3.3 CNFs training

The 128 members of the ensemble serve as training pairs. These pairs are created from the above simulations and consist of a forecasted plume and the associated 4D seismic observation. For the CNF training, we implemented a first-of-its-kind 3D conditional normalizing flow in the open-source package InvertibleNetworks.jl (Orozco, Witte, et al. 2024). Crucially, the scalability of this generative network to 3D volumes was enabled by the memory-frugal invertible layers of the normalizing flow. The network weights ϕ are trained by minimizing the objective equation 3 with ADAM (Kingma and Ba 2014) optimizer and for a total of 120 epochs,

$$\widehat{\phi} = \underset{\phi}{\operatorname{argmin}} \ \frac{1}{M} \sum_{m=1}^{M} \left(\frac{\left\| f_\phi(\mathbf{x}^{(m)}; \mathbf{y}^{(m)}) \right\|_2^2}{2} - \log \left| \det \left(\mathbf{J}_{f_\phi}^{(m)} \right) \right| \right). \tag{3}$$

where $\mathbf{J}$ represents the Jacobian of the network f_θ with respect to its input and M is the number of training samples. For details on the implemenation we refer to (Gahlot et al. 2024).

4 Results

We illustrate the performance of our method on an unseen (not part of the training) plume shown in figure 1b. To calculate posterior statistics, we use 128 posterior samples to calculate the mean and standard deviation. figure 1d shows the inferred plume conditioned on the observed seismic data in figure 1a. figure 1e shows the error between the mean of the posterior and the ground-truth plume in figure 1b. figure 1f shows the uncertainty of the inferred plume. We highlight that there is a good correlation between the error and uncertainty, which is an indication that the uncertainty is well calibrated.

5 Conclusions

We present a 3D Digital Shadow to monitor a 3D time-lapse CO_2 flow using 4D seismic data. Our method introduces a novel implementation of scalable normalizing flows, which facilitates the first known application of generative modeling to realistically sized 3D volumes. The results show significant improvements in CO_2 plume estimates when seismic 4D data was incorporated at the monitoring step, particularly in bringing the predicted plume to the correct shape and size shown in the seismic and ground truth plume. The framework also demonstrates well-calibrated uncertainty quantification, with strong correlations between inferred uncertainty and ground-truth errors. This study confirms that the Digital Shadow, integrating 3D seismic data, effectively tracks CO_2 plume dynamics and lays the groundwork for a 3D Digital Twin to optimize CO_2 storage operations.

6 Acknowledgement

References

E. Jones, C., J. A. Edgar, J. I. Selvage, and H. Crook. 2012. "Building Complex Synthetic Models to Evaluate Acquisition Geometries and Velocity Inversion Technologies." *In 74th EAGE Conference and Exhibition Incorporating EUROPEC 2012*, cp–293. https://doi.org/https://doi.org/10.3997/2214-4609.20148575.

Gahlot, Abhinav Prakash, Rafael Orozco, Ziyi Yin, and Felix J. Herrmann. 2024. "An Uncertainty-Aware Digital Shadow for Underground Multimodal CO2 Storage Monitoring." https://doi.org/10.48550/arXiv.2410.01218.

Kingma, Diederik P., and Jimmy Ba. 2014. "Adam: A Method for Stochastic Optimization." *CoRR* abs/1412.6980. https://api.semanticscholar.org/CorpusID:6628106.

Louboutin, Mathias, Philipp Witte, Ziyi Yin, Henryk Modzelewski, Kerim, Carlos da Costa, and Peterson Nogueira. 2023. "Slimgroup/JUDI.jl: V3.2.3." Zenodo. https://doi.org/10.5281/zenodo.7785440.

Lumley, David. 2010. "4D Seismic Monitoring of CO 2 Sequestration." *The Leading Edge* 29 (2): 150–55.

Møyner, Olav, Grant Bruer, and Ziyi Yin. 2023. "Sintefmath/JutulDarcy.jl: V0.2.3." Zenodo. https://doi.org/10.5281/zenodo.7855628.

Orozco, Rafael, Ali Siahkoohi, Mathias Louboutin, and Felix J. Herrmann. 2024. "ASPIRE: Iterative Amortized Posterior Inference for Bayesian Inverse Problems." https://arxiv.org/abs/2405.05398.
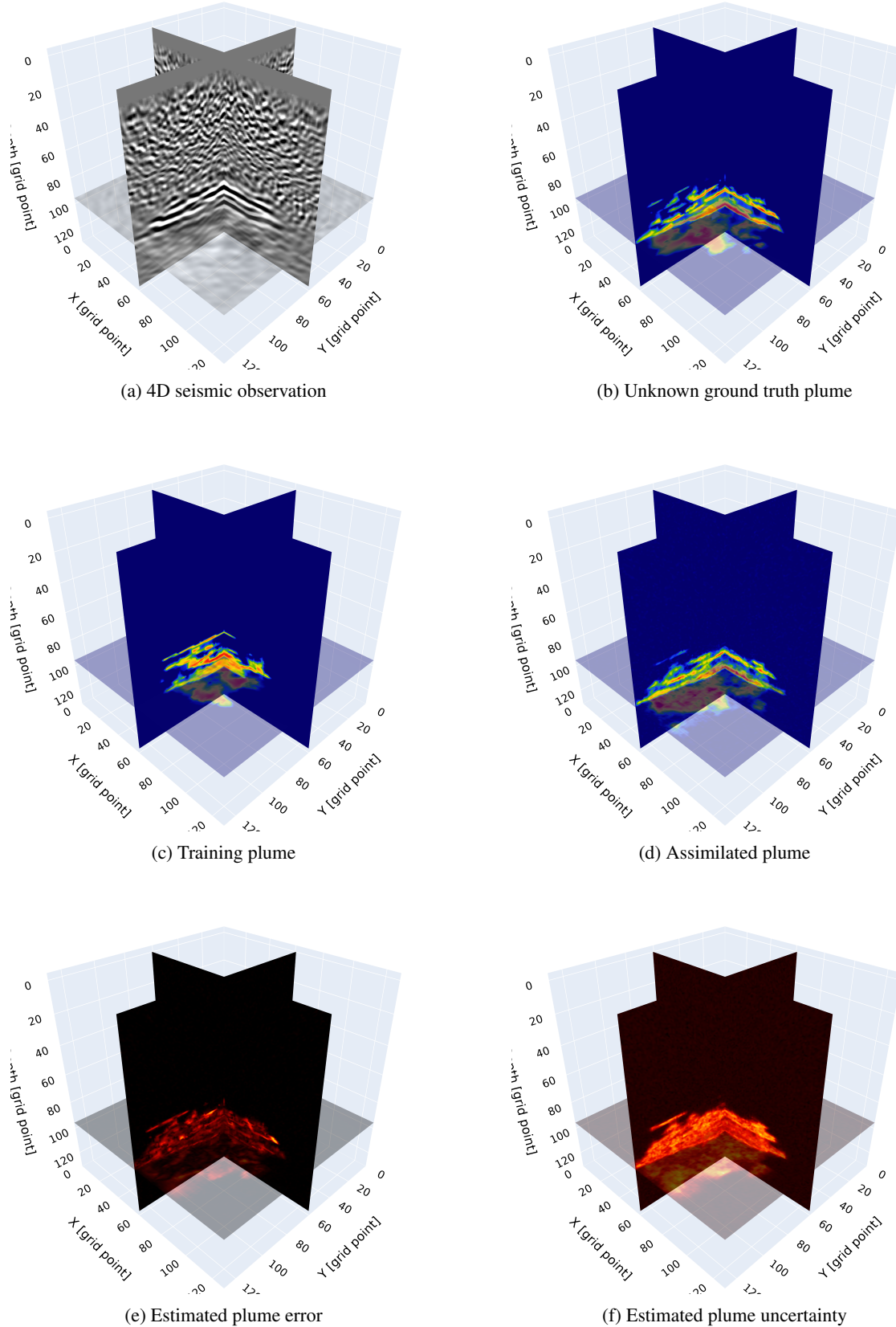
(a) 4D seismic observation

(b) Unknown ground truth plume

(c) Training plume

(d) Assimilated plume

(e) Estimated plume error

(f) Estimated plume uncertainty

Figure 1: *(a)* Time-lapse seismic measurements used as conditioning input to the trained conditional Normalizing Flow. *(b)* The ground-truth unknown plume that is the target to monitor *(c) An ensemble member for the state of the plume used for training.* (d)* A posterior sample conditioned on the seismic observation *(e)* Error between the inferred posterior mean and the ground truth *(f)* The variance between posterior samples.

Orozco, Rafael, Philipp Witte, Mathias Louboutin, Ali Siahkoohi, Gabrio Rizzuti, Bas Peters, and Felix J. Herrmann. 2024. "InvertibleNetworks.jl: A Julia Package for Scalable Normalizing Flows." *Journal of Open Source Software* 9 (99): 6554. https://doi.org/10.21105/joss.06554.

Panel on Climate Change), IPCC (Intergovernmental. 2018. *Global Warming of 1.5° c. An IPCC Special Report on the Impacts of Global Warming of 1.5° c Above Pre-Industrial Levels and Related Global Greenhouse Gas Emission Pathways, in the Context of Strengthening the Global Response to the Threat of Climate Change, Sustainable Development, and Efforts to Eradicate Poverty*. ipcc Geneva.

Papamakarios, George, Eric Nalisnick, Danilo Jimenez Rezende, Shakir Mohamed, and Balaji Lakshminarayanan. 2021. "Normalizing Flows for Probabilistic Modeling and Inference." *J. Mach. Learn. Res.* 22 (1).

Ringrose, Philip. 2020. *How to Store CO$_2$ Underground: Insights from Early-Mover CCS Projects*. Vol. 129. Springer.

———. 2023. *Storage of Carbon Dioxide in Saline Aquifers: Building Confidence by Forecasting and Monitoring*. Society of Exploration Geophysicists.

Spantini, Alessio, Ricardo Baptista, and Youssef Marzouk. 2022. "Coupling Techniques for Nonlinear Ensemble Filtering." *SIAM Review* 64 (4): 921–53.

Witte, Philipp A., Mathias Louboutin, Navjot Kukreja, Fabio Luporini, Michael Lange, Gerard J. Gorman, and Felix J. Herrmann. 2019. "A Large-Scale Framework for Symbolic Implementations of Seismic Inversion Algorithms in Julia." *Geophysics* 84 (3): F57–71. https://doi.org/10.1190/geo2018-0174.1.